THE ASTROPHYSICAL JOURNAL, 270:200–210, 1983 July 1

STELLAR IMAGES DERIVED FROM ROTATION BROADENING: AW URSAE MAJORIS

LAWRENCE ANDERSON AND DARRYL STANFORD
Ritter Observatory, University of Toledo

AND

DOUGLAS LEININGER
Liberty Center High School, Liberty, Ohio
Received 1982 June 28; accepted 1982 December 9

ABSTRACT

We have used observations of the rotation broadening of spectral lines in the W UMa binary AW UMa to derive the star's shape and surface brightness distribution. The assumption that line profiles (continuum normalized) remain uniform over the surface of a rotating star allows one to use a suitably chosen standard profile to deconvolve a Doppler redistribution function. If the star is rotating rigidly, this redistribution function is a one-dimensional spatial image of the star. We tested the uniform-profile approximation for the Mg I *b* triplet at 5170 Å in LTE on a rapidly rotating model contact binary. We found that a Fourier deconvolution of the image-integrated spectrum by a standard flux profile departs from the true continuum redistribution function by only a few percent. Encouraged by this result, we observed AW UMa at many phases and obtained Doppler redistribution functions that were consistently too narrow and asymmetric for the assumed geometry of the system. We conclude that a large fraction of the primary component is covered with a solar-like plage centered on the side away from the secondary, which radically alters the local line equivalent widths.

Subject headings: line profiles — stars: eclipsing binaries — stars: individual — stars: rotation

I. INTRODUCTION

Most of us are very curious to see resolved images of stars other than the Sun. In addition, the information content of full images is potentially large. Examples of global information include shape, limb darkening, gravity brightening, differential rotation, high-order pulsation, and permanent magnetic field distribution. Departures from global phenomena include organized but irregular flow patterns, plages or similar bright regions, and dark spots. Each of these examples can contribute to our understanding of the structure of stars and the theory of stellar atmospheres.

Traditionally, stellar radii have been determined from the light curves of eclipsing binaries, from the formula $L = 4\pi R^2 \sigma T_{\rm eff}{}^4$ coupled with atmosphere models, or from the surface gravity and mass. Of these, the first is the most direct but can be applied to only a limited number of stars. The light and magnetic field *distribution* over stellar surfaces is far more uncertain, having been determined from light curves and changes in Zeeman profiles as a function of rotation phase. These methods suffer from nonuniqueness through the integration of specific intensities over the surface facing the observer. Finally, organized velocity fields other than rotation and winds have not been convincingly resolved on any star other than the Sun. Image synthesis through interferometry promises to be the most direct method of resolving the stars. However, for the immediate future this approach is limited to the few stars of largest angular diameter and even then will resolve only the coarsest detail.

Over fifty years ago Shajn and Struve (1929) developed the theory of rotation broadening of spectral features through a graphical technique which implicitly recognized that the broadening proceeds from the image of the star. Since the interest at the time was stellar rotation, they began with assumed images and adjusted the rotation rate to match observed spectra. One can just as well begin with an observed spectrum and derive the stellar image under the same basic assumptions. Spatial resolution is transformed into velocity resolution, which is distance independent, and the limitation to stars where rotation dominates over other velocity fields is much less restrictive than the limitations on any of the previous methods. In this paper we explore this inversion of a classical problem, and we use the technique to interpret new spectroscopic observations of the W UMa star AW Ursae Majoris. Section II briefly reviews the graphical approach to rotation broadening and states the implicit assumptions. Section III describes the observations and data reduction method. Section IV examines more closely the most important assumption: that the locally emitted spectral profile is uniform over the stellar surface. Section V presents the results for AW UMa, and § VI contains a discussion.

II. ROTATION BROADENING AND THE STELLAR IMAGE

The classical treatment of rotation broadening stems from the fact that contours of constant radial velocity on a rigidly rotating object are parallel to the projected rotation axis, z, and have values proportional to the projected distance perpendicular from the axis, x. The linearity of Doppler shifts suggests we choose velocity $dv = cd\lambda/\lambda$ for the independent spectrum variable. We now define a normalized velocity redistribution function $R(v'; v)dv$ as that fraction of the specific luminosity emitted at v' toward the observer which is shifted to the interval $(v, v + dv)$ in the observer's frame. We prefer the expression *specific luminosity* (Rybicki 1970) over the word *flux* to avoid confusion with the local surface flux $\int I(\hat{n})\hat{n}d\omega$. We may then write the observable specific luminosity at v as

$$H_0(v) = \iint_{\text{image}} I(v - v_r, x, z)dzdx \equiv \int_{-\infty}^{\infty} R(v - v_r; v)H_e(v - v_r)dv_r , \quad (1)$$

where $v_r = v - v'$ is the radial velocity of the image element (x, z), and $H_e(v') = \iint I(v', x, z)dzdx$ is the specific luminosity emitted at v' (the spectrum of a stationary star with the same surface intensity distribution). All specific intensities $I(v', x, z)$ in these and future expressions implicitly include the observer direction and refer to spectral velocities in the frame comoving with element (x, z). Although derived with rigid rotation in mind, this expression for the observed spectrum applies more generally to any surface velocity field. Recovering $R(v - v_r; v)$ from $H_o(v)$ would be equivalent to generating a one-dimensional "spectroastrogram" of the star. Unfortunately, both R and H_e are unknown, so a unique solution in general is impossible (cf. Mihalas 1979).

However, a unique solution is obtained under the condition that $R(v - v_r; v)$ is independent of v (that is, all points in the spectrum suffer the same redistribution). This condition is equivalent to an assumption that $I(v', x, z)$ can be separated: $I(v', x, z) = h(v')g(x, z)$. Here $g(x, z)$ is the normalized ($\iint gdzdx \equiv 1$) stellar image, and $h(v')$ is the locally emitted spectral profile, now equal to $H_e(v')$. The contribution to $H_o(v)$ provided by regions moving at $(v_r, v_r + dv_r)$ becomes

$$R(v - v_r; v)h(v - v_r)dv_r = h(v - v_r)\iint_{v_r} g(x, z)dzdx , \quad (2)$$

where the image integral is restricted to the regions within the radial velocity interval. Thus

$$R(v - v_r; v)dv_r = \iint_{v_r} g(x, z)dzdx \equiv R(-v_r)dv_r .$$

Under this condition, $H_o(v)$ becomes a true convolution $H_o(v) = \int R(-v_r)h(v - v_r)dv_r$ (Carroll 1933; cf. Gray 1976). As such, $R(-v_r)$ can be recovered through standard Fourier deconvolution assuming an appropriate profile $h(v')$. We refer to this condition as the *uniform-profile approximation* in reference to the separation of $I(v', x, z)$. In § IV we examine its validity.

III. OBSERVATION AND DATA REDUCTION

We chose to observe AW UMa because it is a rapidly rotating aspherical object with reasonably well determined geometry. It is also the brightest W Ursae Majoris binary visible from Toledo. Available instrumentation effectively limited observation to about 35 Å of the visible spectrum. We chose to center this window at 5176.62 Å to include the Mg I b triplet $\lambda\lambda$5167, 5173, 5184. These lines are strong but relatively narrow, and contain much spectral information at Fourier wavenumbers similar to those expected in the rotation profile. They are also relatively isolated from other strong lines.

We observed AW UMa with the Ritter 1 m reflector, echelle spectrograph, a Varo two-stage image intensifier, and Kodak 103a-F plates treated with forming gas. The plate dispersion was about 2 Å mm^{-1}. The entrance slit and intensifier degradation gave an effective spectral resolution of about 0.4 Å (200 μm, 25 km s^{-1}). Typical exposure times were 15–30 minutes, or 0.02–0.05 orbital periods. We obtained spectrograms during the 1981 observing season. In the best spectrograms, the signal-to-noise ratio in individual resolution elements was of order 10:1. The largest source of noise was a nonrepetitive pattern in the image intensifier response with characteristic size about 400 μm.

We traced the plates with a modified Gaertner comparator interfaced with an Altair 8800b microcomputer, sampling 1500 points over about 17 mm (35 Å). Because the highly broadened lines are very shallow, the characteristic curve of the emulsion is of secondary importance; we used one curve predetermined from several spot sensitometric plates. For each plate we then (*a*) determined dispersion from adjacent comparison spectra, (*b*) subtracted the adjacent intensifier background (usually less than 10%), (*c*) fitted a fourth-order polynomial to a continuum estimated by eye, (*d*) converted to residual flux units, and (*e*) numerically filtered the result with a Gaussian of half-width 8 km s^{-1} at 1024 positions with equal velocity intervals $\Delta v = 2.071$ km s^{-1}. Figure 1 shows a sample record.

As suggested in the previous section, we derived velocity redistribution functions $R(-v_r)$ through Fourier deconvolution. In the Fourier domain $\tilde{R}(\sigma) = \tilde{H}_o(\sigma)/\tilde{h}(\sigma)$ via the deconvolution theorem. Here σ is measured in s km^{-1}, and the tilde indicates the transform of the non-tilded quantity.

For such a short window of spectrum it is advisable to use a modeled flux profile for the surface-emitted $h(v')$. A synthetic spectrum has only numerical round-off noise, and even the simplest LTE, scaled atmosphere is likely to be as accurate as any choice of nonrotating standard star. Therefore, we synthesized a standard $h(v')$ as described in the next section. This standard was not filtered with the Gaussian.

No attempt was made to account for the leakage of information from one end of the data window into the

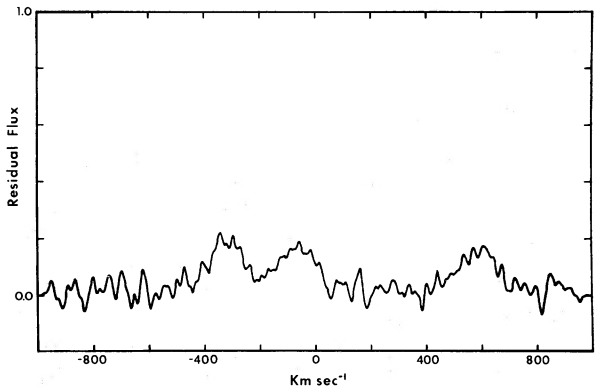

FIG. 1.—The observed residual spectrum of AW UMa at phase 0.86, plate 2103.

other due to the repetitive nature of discrete, finite Fourier transforms. We also ignored the blending of lines outside into the window, because all lines within blending "reach" of the window boundaries are weak. After deconvolving each record with the standard $h(v')$, we applied two forms of smoothing in the Fourier domain. First, because adjacent values of the transform $\tilde{R}(\sigma)$ are correlated, we performed complex averages of three or five adjacent values. This action transforms into the velocity domain as a multiplication by the sinc function and can be removed by an appropriate correction. In the Fourier domain, it significantly reduces the white-noise level, sometimes revealing sidelobes not otherwise apparent. Then, we multiplied by an exponential filter of the form $1/\{\exp[(\sigma - \sigma_o)/\Delta\sigma] + 1\}$. We chose σ_o at the intersection of a linear extension from the average noise at high σ with an average falling signal at low σ (typically $\sigma_o \sim 25$–30 cycles per window $= 0.012$–0.015 s km^{-1}) and $\Delta\sigma \sim 0.2\sigma_o$. This filter has the same cutoff σ_o as the "optimum" filter of Brault and White (1971) but differs in form because we do not wish to assume any particular data function. Figure 2 shows the unsmoothed and smoothed Fourier amplitudes of the tracing in Figure 1 deconvolved with $h(v')$. No attempt was made to remove the instrumental profile as its width in velocity is about $0.3/\sigma_o$.

IV. THE UNIFORM-PROFILE APPROXIMATION

The usefulness of the uniform-profile approximation is well recognized in the literature (cf. Smith and Gray 1976). In general, however, the approximation is *not* strictly valid. The specific-intensity profile of a spectral line varies with emergent angle and local surface gravity even in the simplest of treatments and becomes hopelessly uncertain when chromospheric reversals and/or non-isotropic turbulence are present. Smith (1976) showed that when the large-scale velocities are of the same order as the natural width of a line, convolution is no longer valid. Mihalas (1979) argued that a velocity gradient along the line of sight also invalidates convolution. However, when the Doppler shifts due to tangential surface velocities are large compared with the natural line width, the situation changes. Then, Gray (1975) argued, the observed line shape is controlled by the large-scale velocity structure and not by the local profile. In the Fourier domain, all the information about the velocity field occurs at low σ (s km^{-1}) before the "intrinsic" profile $\tilde{h}(\sigma)$ has changed much from its $\sigma = 0$ value, and thus the detailed nature of $h(v)$ is unimportant. But, the profile shape is only part of the story. If the intensity equivalent width is a strong function of position on the image, convolution, although valid in the sense that its use in spectrum reconstruction tells us something about the velocity field, does not sample the entire star with equal weight. Thus, for example, the v sin i's of rigidly rotating stars derived from weak lines in LTE through deconvolution will be systematically low unless calibrated with theoretical models.

Unless conditions are particularly adverse (thick

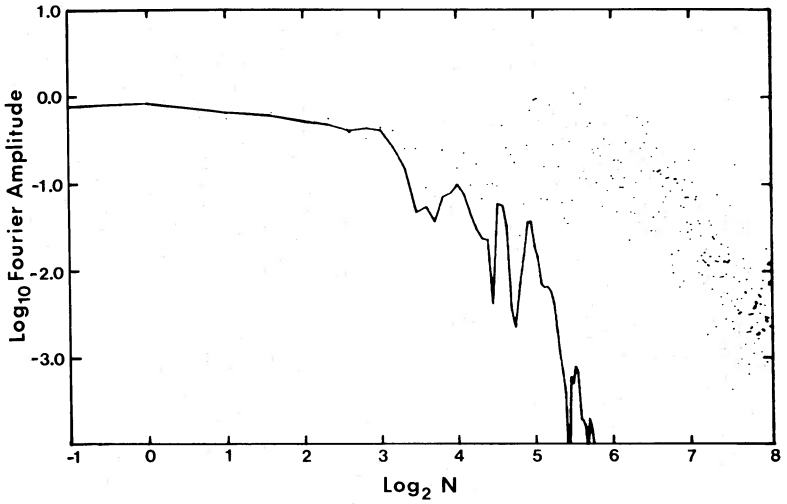

FIG. 2.—The Fourier amplitudes $|\tilde{R}(\sigma)| = |\tilde{S}(\sigma)/\tilde{h}(\sigma)|$ for plate 2103. *Dots*: unfiltered; *solid line*: filtered. The abscissa is the base 2 log of the number of waves per 2121 km s^{-1}. The abscissa labeled -1 represents $\sigma = 0$.

chromospheres, large microturbulence variations, steep velocity gradients), the intensity equivalent widths of strong lines vary less than those of weak lines over the image. We may consider a strong line as a hole in the continuum, so that the observed spectrum is dominated by the continuum redistribution function, which *is* frequency independent over any short interval.

To test the uniform-profile approximation, we synthesized a segment of spectrum emitted by a rigidly rotating model for AW Ursae Majoris. We stress that this model is *not* meant to be a fit to our observations, and was in fact completed before the observations were fully reduced. Rather, its sole purpose was to analyze the influence of two effects expected to be present, gravity brightening and limb darkening. As such, the exact choice of model parameters is unimportant, and application of the result is not limited to the single object AW UMa or even the class of W UMa stars. The test consisted of (*a*) placing on an equipotential surface (in Roche geometry) model atmospheres with effective temperature a prescribed function of the local gravity, (*b*) evaluating the integral in equation (1) at each point in the synthetic spectrum, (*c*) deconvolving the result by the synthetic flux profile of one stationary atmosphere, and (*d*) comparing this deconvolved redistribution function with the direct redistribution of continuum radiation emitted at one frequency. Pertinent model data appear in Table 1. The entries were derived from light curve synthesis models (Mochnacki and Doughty 1972; Lucy 1973) and have been recently confirmed spectroscopically (McLean 1981). The mass and the separation (in velocity units) are the spectroscopic values. Although there is some disagreement on these values (cf. Mochnacki 1981), the model parameters (velocity scale and photospheric surface gravity) are only linearly dependent on the separation, which is probably accurate to 20%. We should note, however, that the separation velocity of 400 km s^{-1} is more than 5 times the "stationary" width of the strongest line modeled or observed. Therefore, Smith's (1976) criterion mentioned at the beginning of this section is well met.

The spectral type of AW UMa (F0–F2) suggests an average effective temperature of about 7000 K. In stars at this temperature, envelope convection is insufficient to redistribute flux over an equipotential surface. Therefore, the Eddington–von Zeipel law of gravity brightening (surface flux $\propto g$) should be appropriate for much of the emergent radiation. The model assumes that all surface elements are independent plane-parallel atmospheres that lie on the locus $T_{\rm eff} \propto g^{0.25}$ passing through $(T_{\rm eff}, \log_{10} g) = (7244\ {\rm K}, 4.3)$. Although about half of the emergent radiation comes from surface elements with local $T_{\rm eff}$ greater than 6500 K, Eddington–von Zeipel gravity brightening causes most of the surface to have local $T_{\rm eff}$ less than 6500 K. The real AW UMa thus may be an interesting borderline case, where large pockets of convective "continent" float on a radiative "mantle." Gravity brightening on the continents would be much less pronounced (Lucy 1967; Anderson and Shu 1977; Eaton, Wu, and Ruciński 1980). If no other effects are present, convection and surface flux distribution presumably adjust to radiate the total luminosity generated in the two cores, with local $T_{\rm eff} \propto g^{0.25}$ in radiative regions, local $T_{\rm eff} \sim 6500$ K in convective regions, and no discontinuity at the boundaries. In fact, light curve synthesis suggests an average gravity-brightening law between the radiative and convective extremes (cf. Woodward, Koch, and Eisenhardt 1980; Hrivnak 1982). Since the purpose of our model is only to check the uniform-profile approximation, we are not concerned with these subtleties, but we will return to this point in § VI.

TABLE 1

HYPOTHETICAL AW URSAE MAJORIS

Parameter	Value
Ephemeris	JD 2,443,980.337 + 0.438732E
Inclination i	79°
Mass ratio q	0.08
Primary mass M_1	2.68 $M_\odot$
Separation	$S = 2.41 \times 10^{11}$ cm, $\Delta v = 400$ km s^{-1}
Primary pole radius	1.33×10^{11} cm
Primary pole $\log_{10} g$	4.3
Primary pole $T_{\rm eff}$	7244 K
Filled fraction[a] f	0.5

[a] Defined as $(C_p - C_1)/(C_2 - C_1)$, where C_p, C_1, C_2 are the potentials of the photosphere and Lagrangian points, L_1, L_2, respectively.

To perform the surface integration, we calculated the emergent specific intensity at five zenith angles from six model stellar atmospheres on the locus having values of $\log_{10} g = 3.3, 3.5, 3.7, 3.9, 4.1, 4.3$. Each atmosphere had a temperature–optical depth distribution scaled proportionally to $T_{\rm eff}$ from Kurucz's (1979) model at $(T_{\rm eff}, \log_{10} g) = (6500\ {\rm K}, 4.0)$ with solar abundances. We assumed LTE for all calculations of level populations and source functions.

We tabulated specific intensities from the models at 255 equal intervals in $\log_{10}$ ($h\nu$ in eV) from 0.37800 to 0.38055, which corresponds to our observed window. The interval, 0.00001, corresponds to a unit velocity interval $\Delta v = 6.903$ km s^{-1}. Nine lines in addition to the Mg triplet were included in the spectral synthesis. Table 2 contains atomic data for all lines. Figure 3 shows the emergent flux profiles, continuum normalized, from the three hottest models. The total equivalent width of non-Mg lines is about equal to that of one Mg line. We estimate that the total equivalent width of lines not included is considerably smaller.

Surface integration proceeded as follows. A square picture plane divided into 73 rows of 121 pixels each was constructed perpendicular to the line of sight in front of the star. Sequential pixels in a row correspond to unit velocity intervals in the spectrum. A probe was extended from each pixel center parallel to the line of sight until it passed or encountered the photospheric equipotential. If it encountered the photosphere, the surface normal, gravity, and emergent angle cosine were determined. Finally, the pixel's contribution to the emergent spectrum, appropriately shifted, was linearly interpolated

TABLE 2

ATOMIC LINE DATA

λ/log$_{10}$ eV	Ion	Mult. No.[a]	log$_{10}$ A_{ul}	log$_{10}$ γ_N	α[b]	β[b]	log$_{10}$ C_4	Ref.
5162/0.38047.....	Fe I	1089	7.26	8.0	0.154	0.32	...	1
5166/0.38014.....	Fe I	1	3.4	8.0	0.038	0.35	...	1
5167/0.38005.....	Mg I	2	7.06	8.0	0.116	0.36	−5.4	2
5167/0.38004.....	Fe I	37	6.39	8.0	0.03	0.32	...	3
5169/0.37992.....	Fe I	1	3.6	8.0	0.038	0.35	...	1
5169/0.37991.....	Fe II	42	5.83	8.4	0.027	0.41	...	4, 5
5172/0.37969.....	Fe I	36	5.68	8.0	0.03	0.32	...	3
5172/0.37969.....	Fe II	35	3.11	8.5	0.027	0.41	...	1
5173/0.37960.....	Mg I	2	7.54	8.0	0.116	0.36	−5.4	2
5184/0.37868.....	Mg I	2	7.76	8.0	0.116	0.36	−5.4	2
5186/0.37849.....	Ti II	86	5.93	8.2	0.033	0.40	...	6
5189/0.37876.....	Ti II	70	6.47	8.0	0.053	0.35	...	6

[a] Moore 1959.

[b] Deridder and van Rensbergen 1976.

REFERENCES.—(1) Kurucz and Peytremann 1975. (2) Gray 1976. (3) Bridges and Kornblith 1974. (4) Phillips 1979. (5) Assousa and Smith 1972. (6) Roberts, Anderson, and Sørensen 1973.

in log$_{10}$ g from the tabulated specific intensities. Velocity information resides in the lines, not the continuum. Therefore, we calculated spectra in terms of residual fluxes: $S(v) = [H_{\rm cont} - H(v)]/H_{\rm cont}$. Figure 4 contains the residual spectra for two rotation phases of the model, plotted with the emergent flux from the tabulated atmosphere 4.1 ($T_{\rm eff}$ = 6457 K).

While summing the pixel contributions, we extracted two complementary "sections" of the convolutions. The first was the spatial image at 5170.07 Å ($v = 55\Delta v$), $I(v - v_r, x, z)$. Since this wavelength is in the richest part of the synthetic spectrum, the resulting "spectro-astrograms" (Figs. 5 and 6) are the most revealing. The approximately concentric discontinuities in brightness are due to the fact that the emergent intensities were not interpolated between tabulated emergent angles. The lines, particularly λ5173, show the increased width associated with lower $T_{\rm eff}$ at lower g and the lack of limb darkening in the cores expected from LTE radiative atmospheres. Small-scale regularities result from the dot pattern and are not part of the image. These images graphically demonstrate the line blending in the spectra of rapidly rotating stars, by showing that many shifted lines contribute to the specific luminosity at one wavelength.

The second convolution section we extracted was the velocity redistribution function in the continuum, $R(v_c'; v) = \int g_c(x, z)dz/\Omega \sin i$, at 5192 Å ($v_c' = -128\ \Delta v$). Since the continuum is essentially invariant over the window, $R(v_c'; v) = R_c(-v_r)$. This function is the object of both the theoretical and observational analyses.

To test our ability to recover $R_c(-v_r)$ from observed spectra, we deconvolved each broadened spectrum in Figure 4 with the flux profile from atmosphere 4.1. Figure 7 shows the Fourier amplitude of the deconvolution at phase 0.25 compared with that of the true redistribution function $R(v_c'; v)$. Figure 8 shows the same comparison in the velocity domain. The difference between the two redistribution functions is in the expected direction: where gravity and local effective temperature are lower than average, the function derived from deconvolution is larger because of the increased equivalent width of the

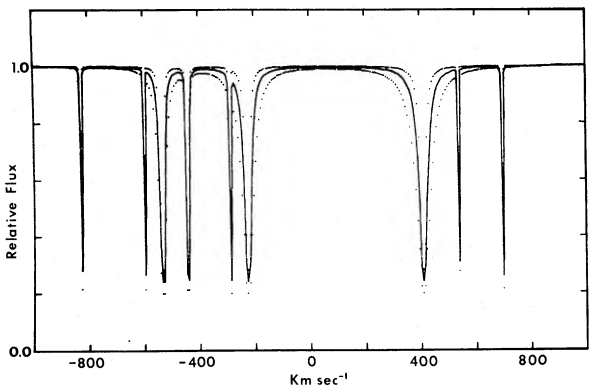

FIG. 3

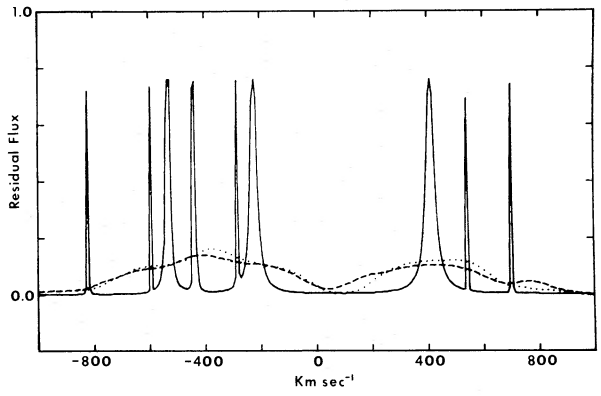

FIG. 4

FIG. 3.—Emergent flux profiles from three atmospheres on the assumed ($T_{\rm eff}$, log$_{10}$ g) locus, continuum normalized. In order of increasing line widths, log$_{10}$ g = 4.3, 4.1, 3.9.

FIG. 4.—Residual spectra for two phases of the model AW UMa, together with that of the flux from the log$_{10}$ g = 4.1 atmosphere

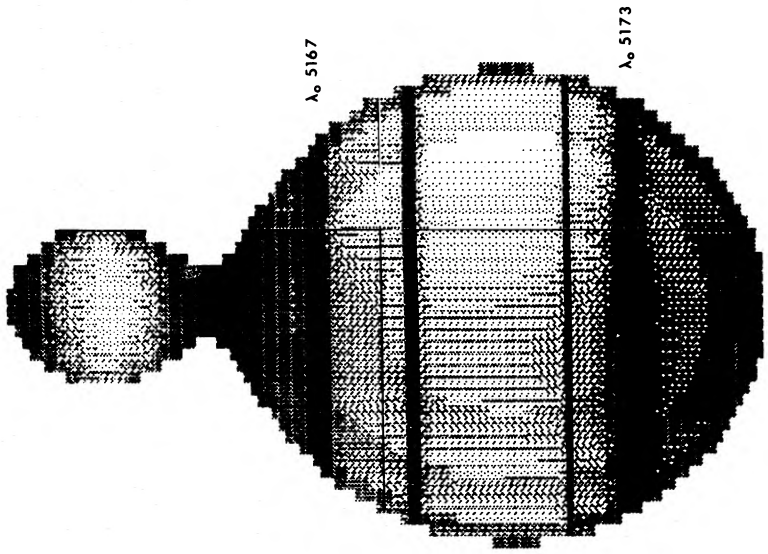

FIG. 5.—The monochromatic image at 5170.07 Å of the model AW UMa at phase 0.25

lines. However, the difference is minimal. At phase 0.0, the deconvolution departed even less from $R(v_c'; v)$.

The results of the above test indicate that we are justified in using deconvolution to recover the stellar image in the velocity domain. In particular, any physically justifiable gravity-brightening law (e.g., convective or some combination of radiative and convective) or limb-darkening law will result in errors less than or equal to the extreme case of the radiative photosphere we chose. We are left with the problem of choosing an appropriate "average" profile $h(v')$. As suggested by Anderson, Raff, and Shu (1980) and McLean (1981), an improper choice (up to $\pm \sim$one-half a spectral class) to first order affects only the normalization and noise, not the overall shape of the redistribution. The most reliable test for $h(v')$ is the total equivalent width of spectral features. The fact that the value of $\tilde{R}(0)$ in the transform domain was very nearly 1.0 without any renormalization shows that atmosphere 4.1 was a fair representation of the total light in the model. We used this atmosphere to synthesize the standard $h(v')$ used to deconvolve the observations.

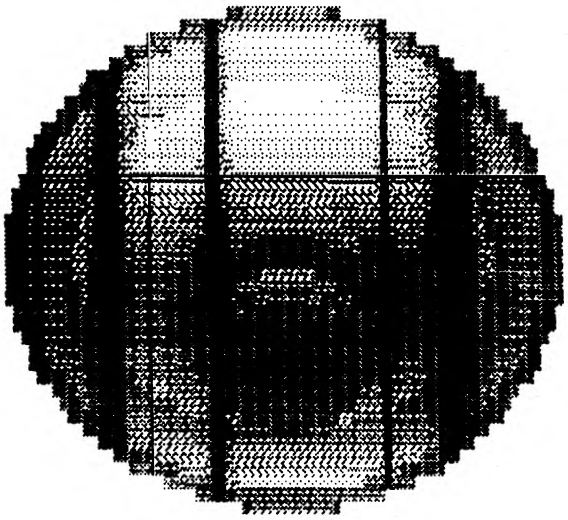

FIG. 6.—The monochromatic image at 5170.07 Å of the model AW UMa at phase 0.0.

In closing this section, we mention that the above treatment is significantly different from the calculations of Anderson and Shu (1979). The above analysis made use of (admittedly somewhat approximate) full atmosphere calculations to determine the emergent specific intensity in an actual spectral window. Anderson and Shu, in order to make their work as broadly applicable as possible, calculated redistribution functions assuming the gray and Eddington approximations and a bolometric weighting of the intensity with local effective temperature. When comparing Figure 8 with an unpublished extension of the Anderson and Shu atlas to mass ratio $q = 0.08$, we found that the relative strength of our secondary component is about 30% larger than that in the atlas. In addition, our primary has relatively more contribution at the limbs. These differences come about because the true continuum at 5192 Å is not as sensitive to the local effective temperature as $T_{\rm eff}^4$.

V. THE OBSERVED REDISTRIBUTION FUNCTIONS

Figure 9 contains the deconvolved velocity redistribution functions for 10 phases of AW UMa. Included on each plot are the expected displacements of the centers of mass of the two components and the expected full width of the primary component in the Roche geometry.

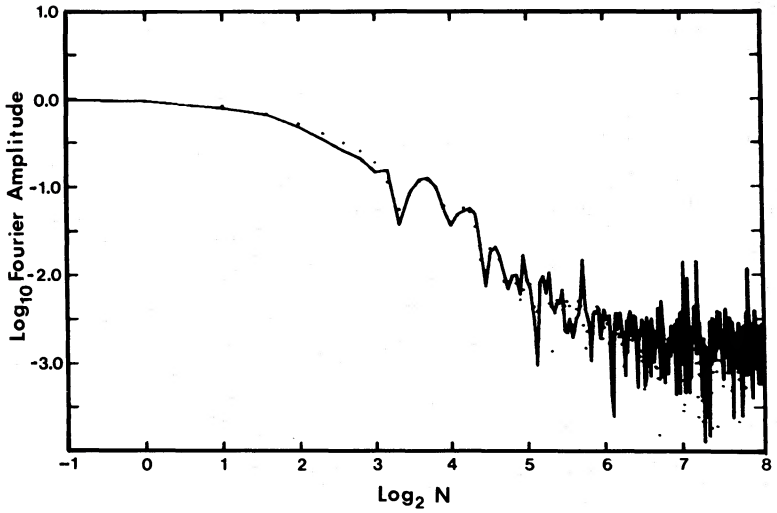

FIG. 7.—The Fourier amplitudes $|\tilde{R}(\sigma)|$ of the theoretical redistribution functions at phase 0.25. *Solid line*: $\tilde{R}_d = \tilde{S}/\tilde{F}_{4.1}$; *dotted line*: true $\tilde{R}_{\text{cont}}$. The abscissa is the base 2 log of the number of waves per 1767 km s^{-1}. The abscissa labeled -1 represents $\sigma = 0$.

On one plot we have included McLean's (1981) profile scaled to the same phase. In general the secondary component is visible where it should be and contributes within a factor of 2 the fraction of the total light expected from the theoretical models of the previous section, 0.12. At all phases, however, the primary component is substantially narrower than the theoretical distribution functions. At elongation the departure is generally asymmetric; light is missing from the side of the primary away from the secondary. At both transit and occultation eclipse the departure is more symmetric. In the affected regions, the light is almost completely absent; $R(-v_r)$ drops to near zero within a velocity interval unresolved by our noise filter. Although one cannot discern its form in the raw spectra, the decreased width of $R(-v_r)$ is apparent in a comparison of Figures 1 and 4.

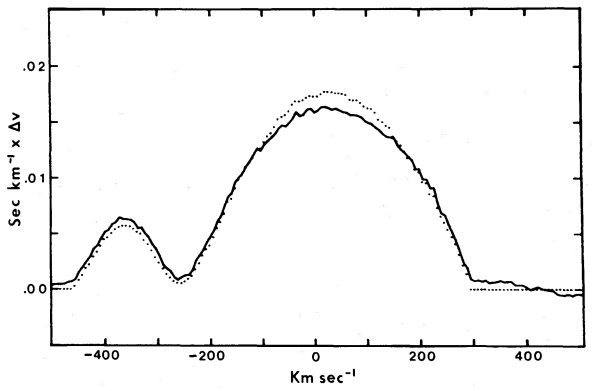

FIG. 8.—The theoretical redistribution functions in the velocity domain at phase 0.25. *Solid line*: $R_d = S$ deconvolved by $F_{4.1}$; *dotted line*: true R_{cont}.

To distinguish among possible explanations for the departures, it is useful to know whether the "missing light" is really missing or is appearing somewhere else in $R(-v_r)$. This information is contained in $\tilde{R}(0)$, the ratio of total equivalent width of lines in the observed spectrum to the width in model 4.1, as a function of phase. Figure 10 shows the phase dependence of $\tilde{R}(0)$. The absolute value of $\tilde{R}(0)$ depends on the choice of deconvolution standard and thus is subject to an error in spectral type of the standard. However, relative variations over phase are not subject to this error. The quantity $\tilde{R}(0)$ is very sensitive to the continuum normalization, which may vary from plate to plate. Most reduced $\tilde{R}(\sigma)$'s were similar to the one shown in Figure 2, in that the first four to six wavenumbers showed only a slowly decreasing $\tilde{R}$ with increasing σ, as predicted by the model. A misplaced continuum would decrease the correlation between these values. The fact that $\tilde{R}(0)$ is approximately 1 at maximum is also an indication that we have chosen an appropriate standard for deconvolution. Thus we are confident that the derived equivalent widths are accurate to within the subjective error bar on Figure 10.

VI. DISCUSSION

We have shown that under certain conditions one may retrieve a star's continuum Doppler redistribution function through the Fourier deconvolution of broadened strong lines by a standard flux profile. Smith's (1976) criterion that the Doppler shifts must be greater than the local line widths may be interpreted as a limit on the velocity resolution one can expect from this procedure. The other condition is that the surface variation of the local line profile be no more than that expected from static, radiative, center-to-limb effects and

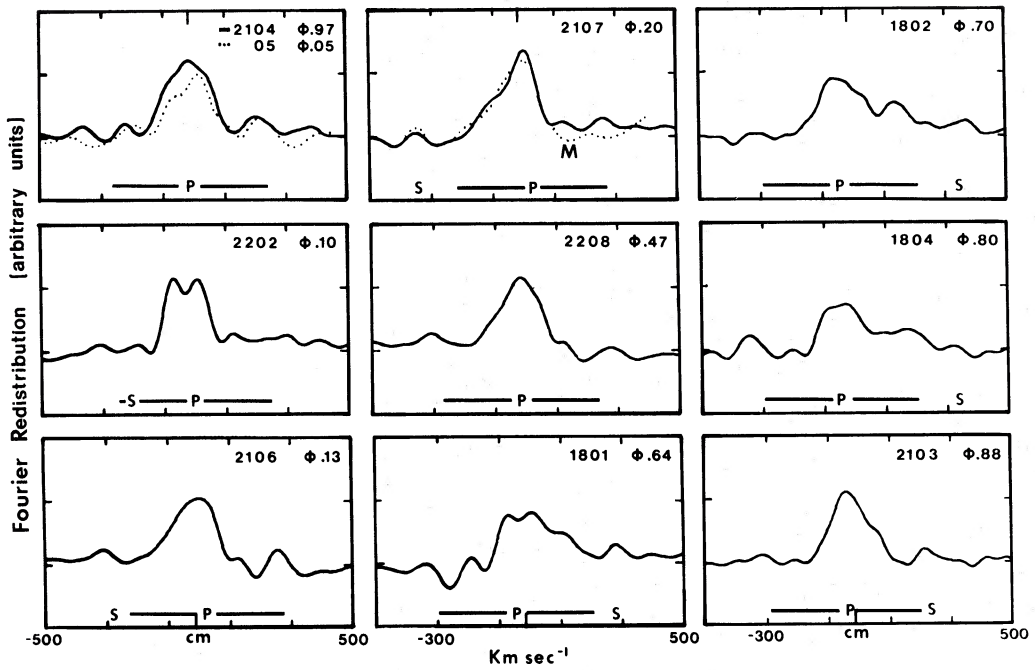

FIG. 9.—Deconvolved velocity distribution functions at 10 phases of AW UMa. *P* and *S* refer to expected displacement of the primary and secondary centers of mass, respectively. The bar indicates the full width of the primary Roche lobe. The dotted curve on plate 2107 is from McLean (1981), scaled to the same phase.

gravity brightening. Since the continuum redistribution function is nearly frequency independent, it represents a one-dimensional map of the continuum surface brightness of the star. For rigid rotation, this map has a simple Euclidean geometry. These very powerful results have previously been recognized but, to our knowledge, not thoroughly tested except in limited application to the determination of rotational velocities and the separation of various velocity-broadening mechanisms (cf. Gray 1976). Keeping the limitations in mind, we now try to understand why our observed deconvolutions do not look like the theoretical redistribution functions.

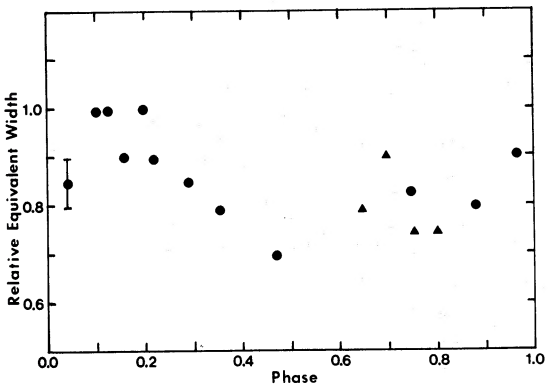

FIG. 10.—Variations with phase of $\tilde{R}(0)$, the ratio of the total equivalent line width observed to that of atmosphere $\log_{10} g = 4.1$. *Circles*: 1981 July; *triangles*: 1981 August.

First, the presence of the secondary in the spectrum argues very strongly for good thermodynamic contact between the stars. Separate stars of such disparate mass would have very different surface fluxes, in the sense that the secondary would seem black by comparison even if the system is evolved. Its correct (within about a factor of 2) contribution in proportion to the continuum-weighted cross sections of the Roche lobes strengthens the argument further and also suggests that most luminous surface elements of each star are contributing their fair share. Although this latter conclusion is not incontrovertible, it can be used to help limit possible explanations for the anomalous line shape of the primary component. Such explanations fall into three classes: departures from rigid rotation, surface variations in continuum brightness, and surface variations in intensity equivalent width.

Nonrigid rotation simply alters the redistribution function without changing the total integral $\tilde{R}(0)$. We can dismiss this explanation on both theoretical and observational grounds. The observed departures would require that a large fraction of the surface of the primary be stationary or even moving in a retrograde direction in the observer's frame. Since the velocities implied are of the order of 30 times the surface sound speed, this explanation seems highly unlikely, particularly as there is no evidence for the accompanying shock heating. One might argue that the primary is not in synchronous

rotation. However, the asymmetry of the redistribution profile suggests that at least the part of the primary facing the secondary is tidally locked. Therefore, any asynchronism would lead to considerable shock heating and dissipation. Finally, if differential rotation alone were present, we would not expect to see the observed phase variation of the total equivalent width of the lines.

One of the purposes of our continuing observations of W UMa stars is to search for surface brightness anomalies in the velocity redistribution functions. Dark spots have been advanced to explain photometric waves in another class of close binaries, the RS CVn stars (cf. Hall 1976), and the fact that occultation minima are deeper than transit minima in the light curves of W-type W UMa stars (Mullan 1975; Anderson and Shu 1977). Such spots must compete against the entire visible surface of the star to be visible photometrically, but they must only compete with other portions of the star at the same velocity to be visible in $R(-v_r)$. If the rotation is rigid, the shape of a depression in $R(-v_r)$ reveals a spot's position and extent in longitude, and its phase dependence can potentially reveal the latitude. Have we found a dark spot on AW UMa that extends from about $-60°$ to $+60°$ in latitude and more than halfway around the star in longitude, centered on the back of the primary? One observation argues strongly against this interpretation. Such a large spot would noticeably depress the occultation minimum in AW UMa's light curve. Since the light curve is not unusual and the mass ratio determined from light curve synthesis agrees with that from spectroscopy without requiring a large temperature difference between the components, a dark spot is unlikely.

The third possibility is that the areas where $R(-v_r)$ goes to zero are indeed radiating in the continuum but are producing absorption lines with equivalent width much smaller than expected. This explanation is in strong violation of the uniform-profile approximation; however, a simple formulation shows that deconvolution is still appropriate. Assume the specific intensity in the continuum is given by $I_c(v, x, z) = hg(x, z)$ with $\iint g(x, z)dxdz = 1$, and in a line by $I_l(v, x, z) = hg'(x, z)$ with $\iint g'(x, z)dxdz = \beta$, and the line has a rectangular profile with constant boundaries at $v = a, b$. It then can be shown that the normalized, observed spectrum is given by

$$S(v) = \frac{H_c - H(v)}{H_c} = \int_{a-v}^{b-v} \left[\iint_{v_r} (g - g')dxdz \right] dv_r , \quad (3)$$

where again the surface integral is performed over the regions of the image moving in the interval $(v_r, v_r + dv_r)$. This expression is simply the convolution of a square emission line with a redistribution function given by

$$R(-v_r)dv_r = \iint_{v_r} (g - g')dzdx .$$

Thus as long as the absorption lines are sufficiently narrow that we do not care about their detailed profile, we may interpret large differences between a deconvolved redistribution function and the continuum redistribution expected for the geometry as a variation of equivalent widths. *Without the additional information provided by light curves or the phase variation of the total equivalent width, we cannot distinguish between dark spots and filled-in absorption lines.*

In § IV we suggested that distorted stars such as AW UMa near the cool limit of radiative photospheres would develop convective "continents" driven by the radiative gravity brightening of their envelopes. We propose that a thick chromosphere overlies much of the convective region on the surface of the primary of AW UMa, in effect a large-scale plage. The current view of chromospheric activity arising from the interaction of convection and rotation leads to this possibility. On the Sun, plages are usually precursors of spot groups; where are the spots on AW UMa? Spots on this star may in fact be very small or nonexistent. The convective regions are very shallow. They exist only to provide the flux diversion required for gravity brightening. As we argued in § IV, the near-zero gravity-brightening exponent in convective regions implies that the convection is at the minimum level required to sustain a constant local effective temperature ~ 6500 K. Such a thin convective zone would not be able to generate or hold against buoyancy large magnetic fields (Parker 1975). The field generated may rise quickly to the surface and float off the star, maintaining a "permanent" plage state. Is it a coincidence that the chromosphere is opaque enough to erase almost exactly the absorption features in the spectrum? One cannot argue that the particular physics of the Mg *b* transitions is responsible, because the same redistribution function was observed by McLean (1981) in a very different part of the spectrum. We suggest that the chromosphere itself acts as a radiant thermostat. At least some absorption in weak lines and the wings of strong lines must be present from an atmosphere in LTE with an outward-directed net radiative flux. A thick chromosphere will back-warm the layers below it until such an outward flux is established. In addition, the back-warming of the already minimum convection may weaken the chromospheric energy source.

The phase variation of the total equivalent width of lines (Fig. 10) is in the direction expected for a plage covering the convection region over 200–250 degrees of longitude on the primary, centered at phase 0.5. We can only speculate at this time that the presence of the secondary inhibits plage formation through either a modification of equatorial circulation patterns or a damping of convection itself, possibly via external irradiation.

Finally, *International Ultraviolet Explorer* observations of AW UMa provide direct evidence for chromospheric activity. Dupree and Preston (1980), Ruciński and Vilhu (1982), and Eaton (1983) all report that this and other A-type W UMa stars exhibit surface fluxes in selected ultraviolet emission lines of chromospheric and transition zone origin about 200 times the solar flux in the same lines, just as do their cooler W-type counter-

parts and the RS CVn stars. The "classical" theoretical distinction between A-type (which have deeper transit minima and are generally of spectral type earlier than F5) and W-type (which have deeper occultation minima and are generally later than F5) W UMa stars is that the former have radiative envelopes, and the latter, convective envelopes. That distinction alone is not enough to cause the observed light curve differences between the two types, although it works in the right direction (Anderson and Shu 1977). However, the ultraviolet evidence and low variations in color (Wilson and Devinney 1973; Eaton 1977; Twigg 1979) suggest that convection is present and provides magnetohydrodynamic heating and decreases gravity brightening even on A-types (Eaton 1983 and Wilson quoted therein). Eaton adds that the presence of convection in A-types argues against Shu, Lubow, and Anderson's (1976, 1979) contact discontinuity model for the interiors of contact binaries. In that model, the separate luminosities generated in the cores are mixed in a thin baroclinic zone lying at the inner critical Roche surface, while the outer common envelope remains barotropic with properties identical to corresponding envelopes in single stars: e.g., the subphotosphere of an early F or late A contact binary should be radiative. However, his argument does not take into account the convective "continents" resulting from *radiative* gravity brightening, which persist well into the A spectral class for the rapidly rotating W UMa stars.

Eaton (1983) closes his paper with the suggestion that the two types of W UMa stars *are* distinguished by the presence (W) or absence (A) of magnetic spots, and asks why the spots should cease to exist earlier than F5 when convection continues well into the A's. We suggest that the answer lies in the "continents." In the A-type stars these "continents," while too thin to support spots, can and do generate the magnetohydrodynamic energy needed to heat a corona and chromosphere. As one moves to stars with later spectral type, the "continents" grow (always remaining thin and having local effective temperatures near 6500 K) until finally, at F5, the entire star is enveloped in convection. Only then can the convection deepen with still later spectral type, and spots appear. This suggestion has two observational tests. First, since there would be no spots on the "continents," one would expect no large flares and a far more constant ultraviolet emission for the A-type W UMa stars. Second, on stars of the earliest spectral type (e.g., AG Vir, V535 Ara, S Ant) one would expect the "continents" to be confined to the very ends of the contact configuration, resulting in periodic modulation of the ultraviolet emission.

Obviously, the ideas and observational technique presented here should be explored with data of higher signal-to-noise ratio. We also suggest that light curve synthesis programs be altered to include the possibility of two gravity-brightening laws with known exponents but unknown fractional area of the star.

We are particularly indebted to Scott Smith and Paul Noah for their advice and assistance with the two-stage image tube and the programming of the minicomputer controlling the densitometer. George Collins suggested the test of the uniform-profile approximation. We also thank Nancy Morrison and Bernard Bopp for helpful comments on the manuscript and Joel Eaton for an advance copy of his manuscript. A referee raised the suggestion of including "continents" in light curve synthesis. Finally, we appreciated support from NSF through the Student Science Training Program in Scientific Research (D. L.), the Faculty Research Award program of the University of Toledo (L. A.), the University of Toledo Graduate School, and the Ritter Publication Fund.

REFERENCES

Anderson, L., Raff, M., and Shu, F. H. 1980, in *IAU Symposium 88, Close Binary Stars: Observations and Interpretation*, ed. M. J. Plavec, D. M. Popper, and R. K. Ulrich (Dordrecht: Reidel), p. 485.
Anderson, L., and Shu, F. H. 1977, *Ap. J.*, **214**, 798.
———. 1979, *Ap. J. Suppl.*, **40**, 667.
Assousa, G. E., and Smith, W. H. 1972, *Ap. J.*, **176**, 259.
Brault, J. W., and White, O. R. 1971, *Astr. Ap.*, **13**, 169.
Bridges, J. M., and Kornblith, R. L. 1974, *Ap. J.*, **192**, 793.
Carroll, J. A. 1933, *M.N.R.A.S.*, **93**, 478.
Deridder, G., and van Rensbergen, W. 1976, *Astr. Ap. Suppl.*, **23**, 147.
Dupree, A. K., and Preston, S. 1980, in *The Universe at Ultraviolet Wavelengths*, ed. R. D. Chapman (NASA CP-2171), p. 333.
Eaton, J. A. 1977, *Bull. AAS*, **9**, 433.
———. 1983, *Ap. J.*, **268**, 800.
Eaton, J. A., Wu, C.-C., and Ruciński, S. M. 1980, *Ap. J.*, **239**, 919.
Gray, D. F. 1975, *Ap. J.*, **202**, 148.
———. 1976, *The Observation and Analysis of Stellar Photospheres* (New York: Wiley-Interscience).
Hall, D. S. 1976, in *IAU Colloquium 29, Multiple Periodic Variable Stars*, ed. W. S. Fitch (Dordrecht: Reidel), p. 287.
Hrivnak, B. J. 1982, *Ap. J.*, **260**, 744.
Kurucz, R. L. 1979, *Ap. J. Suppl.*, **40**, 1.
Kurucz, R. L., and Peytremann, E. 1975, *Smithsonian Ap. Obs. Spec. Rept.*, No. 362.
Lucy, L. B. 1967, *Zs. Ap.*, **65**, 89.
———. 1973, *Ap. Space Sci.*, **22**, 381.
McLean, B. J. 1981, *M.N.R.A.S.*, **195**, 931.
Mihalas, D. 1979, *M.N.R.A.S.*, **189**, 671.
Mochnacki, S. W. 1981, *Ap. J.*, **245**, 650.
Mochnacki, S. W., and Doughty, N. A. 1972, *M.N.R.A.S.*, **156**, 51.
Moore, C. E. 1959, *NBS Tech. Note*, Vol. **36**.
Mullan, D. J. 1975, *Ap. J.*, **198**, 563.
Parker, E. N. 1975, *Ap. J.*, **198**, 205.
Phillips, M. M. 1979, *Ap. J. Suppl.*, **39**, 377.
Roberts, J. R., Anderson, T., and Sørensen, G. 1973, *Ap. J.*, **181**, 567.
Ruciński, S. M., and Vilhu, O. 1982, preprint.
Rybicki, G. B. 1970, in *Spectrum Formation in Stars with Steady-State Extended Atmospheres*, ed. H. G. Groth and R. Wellman (NBS Spec. Pub. No. 332), p. 87.
Shajn, G., and Struve, O. 1929, *M.N.R.A.S.*, **89**, 222.
Shu, F. H., Lubow, S. H., and Anderson, L. 1976, *Ap. J.*, **209**, 536.
———. 1979, *Ap. J.*, **229**, 223.

Smith, M. A. 1976, *Ap. J.*, **208**, 487.
Smith, M. A., and Gray, D. F. 1976, *Pub. A.S.P.*, **88**, 109.
Twigg, L. W. 1979, *M.N.R.A.S.*, **189**, 907.
Wilson, R. E., and Devinney, E. J. 1973, *Ap. J.*, **182**, 539.
Woodward, E. J., Koch, R. H., and Eisenhardt, P. R. 1980, *A.J.*, **85**, 50.

LAWRENCE ANDERSON and DARRYL STANFORD: Ritter Observatory, University of Toledo, Toledo, OH 43606

DOUGLAS LEININGER: 606 Maple Street, Liberty Center, OH 43532